Platinum Nanoparticles Synthesis by Sonoelectrochemical Methods

LAURA OBREJA[1]*, DANIELA PRICOP[1], NECULAI FOCA[2], VIOREL MELNIG[1]
[1] "Al. I. Cuza" University, Faculty of Physics, 11A Carol I Blvd., 700506, Iasi, Romania
[2] "Gh. Asachi" University, Faculty of Chemistry, 71A D. Mangeron Blvd., 700050, Iasi, Romania

Platinum nanoparticles with sizes between 10 and 42 nm have been obtained by a sonoelectrochemical method in the presence of a water-soluble polymer, poly(amidehydroxyurethane) (PAmHU), which acted as a coating agent. The PAmHU stabilized Pt nanoparticles were characterized by X-ray diffraction (XRD), atomic force microscopy (AFM), UV-Vis and FTIR spectroscopy and dimension distribution and Zeta potential analysis. The analyses showed the fact that these nanoparticles are capped by the polymer, which confers them water-solubility and stability.

Keywords: platinum nanoparticles, poly(amidehydroxyurethane), sonoelectrochemical synthesis

In the last years, an increasing interest has been observed regarding the synthesis and characterization of colloidal noble metal nanoparticles because of their unique properties and promising applications. The nanoparticles have a characteristic large surface-to-volume ratio, and consequently a high fraction of the metal atoms exposed at the surfaces. The applications of noble metals nanoparticles include catalysis [1], data storage systems, new electronic devices [2], electrochemical chemo- and biosensors [3], and refractometric and fluorescent sensors [4].

The preparation of colloidal metals with desirable properties represents a significant challenge. The metal nanoparticles can be obtained by several methods such as chemical reduction [5, 6], UV photolysis [7], thermal decomposition [8], metal vapor deposition [9], reduction by ionizing radiation [10], electrochemical synthesis [11] and sonochemical reduction [12].

Many practical applications require platinum nanoparticles to be dispersible in water and preserve their physicochemical properties over a long time. Platinum nanoparticles have been prepared previously in the presence of different stabilizers including polymers [13, 14] (poly(vinyl alcohol), poly(vinylpyrrolidone), poly(*N*-isopropylacrylamide)) and surfactants[15] (sodium dodecyl sulfate), which prevent the nanoparticles from aggregation and allow their isolation.

In a previous paper [12] we reported the platinum nanoparticles sonochemical synthesis by reduction of chloroplatinic acid with methanol, ethanol and propanol in the presence of different capping polymers: chitosan, polyethylene glycol and poly(amidehydroxyurethane).

In this paper it is presented the synthesis and characterization of platinum nanoparticles capped with poly(amidehydroxyurethane) (PAmHU) water-soluble polymer obtained by sonoelectrochemical method. The advantage of this method is that the size control of nanoparticles is tuned by the current monitoring in the galvanostatic process and the restriction reaction room by the polymer microdomain.

Experimental part

Materials and methods

Chloroplatinic acid, sodium carbonate and sodium bicarbonate were purchased from Sigma Aldrich. Details regarding PAmHU synthesis and characterization are given in [16]. All solutions were prepared with Milli-Q water (18.2 MUΩ . cm).

The electrosynthesis was performed in galvanostatic regime. As working (WE) and counter electrode (CE) were used two coiled platinum wires of 160 mm length and 1 mm diameter and 140 mm length and 1.5 mm diameter, respectively. The distance between electrodes was of 1.5 mm and kept the same for all the experiments. The electrodes were cleaned by immersion in chromic mixture, sonicated in distilled water and dried before every usage. A 10^{-3}M solution consisting in chloroplatinic acid and 0.1% *w/w* PAmHU was used as electrolyte solution. The pH of electrolyte solutions was adjusted to 10 with a sodium carbonate and bicarbonate mixture. The galvanostatic regime current density was preset within 0.6 and 1.2 mA/cm^2 using an Amel model 459 potentiostat. The current domain was determined from voltammogram characteristic obtained in a three electrode mode (potentiostatic regime). The working and counter electrode were the same as those used in the synthesis process and the reference electrode was a standard calomel electrode (*sce*), measurements being carried out in the chloroplatinic acid and polymer precursor solution. The optimum time for synthesis was one hour. The synthesis of platinum nanoparticles was performed at room temperature under nitrogen atmosphere and ultrasound stirring (10% amplitude mode at 20 kHz ± 500 Hz standard frequency; Sonoplus-Bandeline set-up).

The characterizations of Pt nanoparticles-PAmHU systems were done in solutions, powders and thin films.

The powders containing Pt nanoparticles were obtained by solutions lyophilisation after sonoelectrochemical synthesis.

The thin film samples were prepared by spin coating method, using a WS-400B-6NPP/LITE spin coater, being deposited on microscope slide glass substrates with 25x25 mm^2 area. The detailed protocol for cleaning glass substrates was presented elsewhere [11].

Characterization methods

The sample powder X-ray diffractograms were recorded in θ - 2θ mode, between 35° and 90° in a Shimadzu XRD 6000 diffractometer with a X-ray generator (CuK_α radiation, λ= 1.54060 Å) operated at 40 kV and 30 mA.

* email: obrejalaura@yahoo.com

The crystallite size was determined from X-ray diffractograms according to Scherrer relationship [17]:

$$L = \frac{K\lambda}{\beta \cos\theta}, \quad (1)$$

where:

L is the dimension of crystallite;

K - a constant (0.89);

β is the half maximum profile line width,

θ - the diffraction angle;

λ - the X-ray wavelength (in our case 1.54060Å).

Atomic Force Microscopy (AFM) analyses were performed in semicontact mode, with a NT-MDT Solver Pro 7M apparatus on thin films.

The dimension of PAmHU capped nanoparticles and Zeta potential were evaluated with a Malvern zetasizer nano SZ at room temperature.

FTIR spectra were recorded on a Tensor 10 Bruker spectrophotometer over the wavenumber range 4000 – 400 cm^{-1}.

The optical properties were studied in solution by exploring the UV-Vis absorption spectra in the 190-850 nm range using a Hitachi Model U – 2010 Spectrophotometer.

The light scattering spectra due to surface plasmon resonance effect characteristic to metallic nanoparticles, which is quantized by nanoparticles size, were simulated with MiePlot v4 software [18] that uses Mie theory. The refractive index of chloroplatinic acid and PAmHU solution was determined at room temperature with an Abbe refractometer, and the platinum refractive index dependence of wavelength was taken from RefractiveIndex.INFO database [19].

Results and discussions

Figure 1 shows the cyclic voltammogram for the electrolyte solution. Cyclic voltammetry (CV) measurements were carried out in a conventional three-electrode assay at the room temperature. The potential has been swept between -1.5V and +1.5V vs. *sce* with a rate of 20mV/s. From this study it results that the optimum values of current density for galvanostatic electrosynthesis are between 0.6 and 1.2 mA/cm^2 dissolution domain.

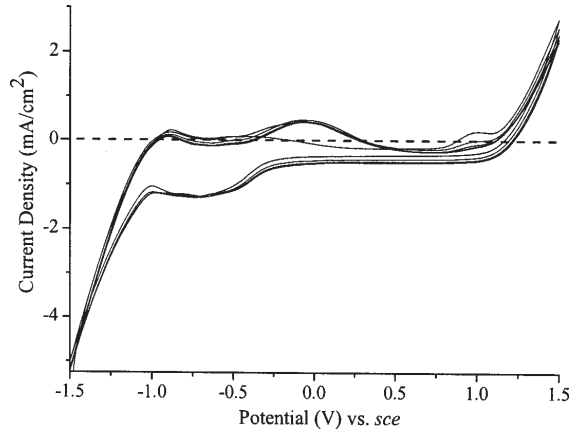

Fig. 1 Cyclic voltammogram for Pt/PAmHU$_{aqua}$-$H_2[PtCl_6]$/Pt system

Taking into account theses results, the sonoelectro-chemical synthesis of platinum nanoparticles was performed in galvanostatic regimes at 0.6, 0.8, 1 and 1.2 mA/cm^2 preset current densities.

After an induction period of 5 min, the solution changed colour from light yellow to orange, becoming colourless at the end of synthesis and grey light after a month.

The reduction of chloroplatinic acid at Pt(0) is confirmed by UV-Vis spectra showed in figure 2. The precursor

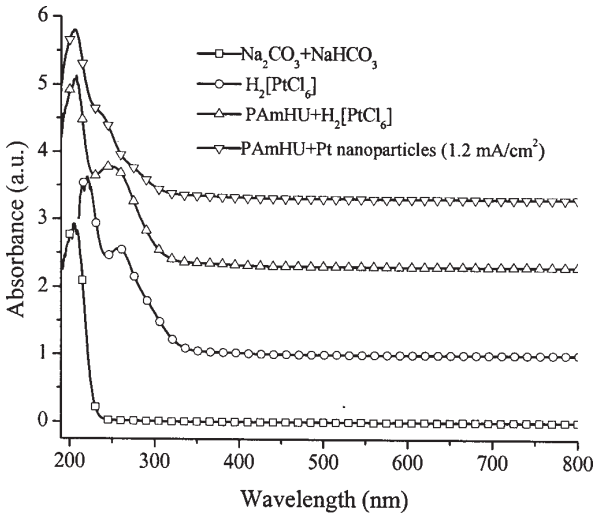

Fig. 2 The UV-Vlis spectra of aqueous precursor solution: sodium carbonate and bicarbonate mixture; chloroplatinic acid; chloroplatinic acid and PAmHU solution and PAmHU-Pt nanoparticles system (obtained at 1.2 mA/cm^2 galvanostatic current)

aqueous solutions and PAmHU-Pt nanoparticles possible system spectra were recorded for comparison.

In the case of chloroplatinic acid, it can be observed a band at 220 nm corresponding to $[PtCl_4]^{2-}$ complex and three ligand-to-metal charge transfer (LMCT) characteristic bands of $[PtCl_6]^{2-}$ complexes, one with a maximum at 262 nm and other two bands at around 360 and 480 nm corresponding to d-d transitions [20, 21], which are slightly solvent dependent and are not observed in our solution. The characteristic values of $[PtCl_4]^{2-}$ and $[PtCl_6]^{2-}$ peaks are slightly shifted to blue due to the presence of PAmHU in aqueous solution.

The PAmHU-Pt nanoparticles possible system spectrum (figs. 2 and 3) show that while the characteristic absorption band for at 262 decreases significantly, the characteristic band for at 220 nm disappear and two new bands at 206 nm and 274 nm, respectively, appear.

To verify if these bands are due to light scattering caused by surface plasma resonance characteristic to metallic nanoparticles, the light scattering spectra were simulated using Mie theory. In figure 3 this simulated spectrum is shown comparatively with deconvoluted UV – Vis spectrum for PAmHU – Pt nanoparticles systems, for the same experimentally measured parameters (367 nm size value of nanoparticles of the most intense peak (determined by DLS) and refractive index of chloroplatinic acid and PAmHU solution at room temperature of 1.3325). The results are convincing proving the existence of Pt nanoparticles and are in good agreement with those obtained in literature for light scattering spectra simulation of Pt nanoparticles using Mie theory [22], even if the sphere determined by DLS analysis is not made only of platinum – as the data were introduced in light scattering simulation.

A possible two-step reaction mechanism can be proposed and sustained by the followings. The standard redox potential of the two ions shows that the reduction of $[PtCl_4]^{2-}$ is more rapid than that of $[PtCl_6]^{2-}$, as would be expected from the standard redox potential of the two ions, i.e., 0.68 V for $[PtCl_6]^{2-}$/ $[PtCl_4]^{2-}$ and 0.755 V for $[PtCl_4]^{2-}$/ Pt(0) (*vs*. the normal hydrogen electrode) [23]. Also, investigation of $[PtCl_6]^{2-}$ alcoholic reduction process by NMR techniques [24], revealed that Pt(0) is not found to occur until a high concentration of Pt(II) (~90% yield of $[PtCl_4]^{2-}$) has been accumulated.

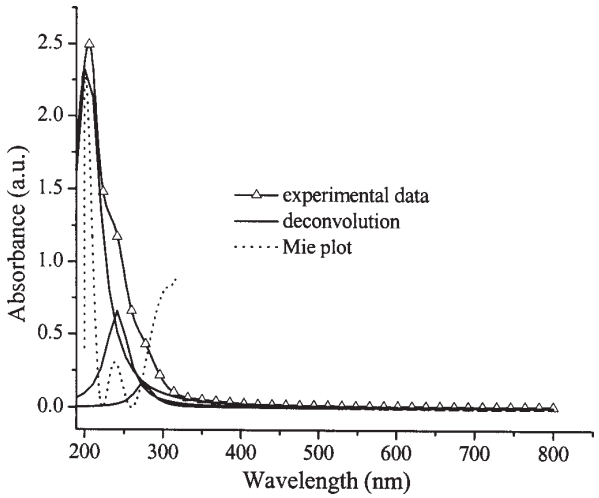

Fig. 3 Deconvoluted UV-Vis spectrum for PAmHU – Pt nanoparticles systems (obtained at 1.2 mA/cm^2 galvanostatic current) and simulated light scattering spectrum (surface plasma resonance) according to Mie theory

To sum up, the precursor for electrochemical synthesis was obtained by the following reactions in electrolyte solution:

$$H_2[PtCl_6] \leftrightarrow 2H^+ + [PtCl_6]^{2-}$$

$$[PtCl_6]^{2-} \xleftrightarrow{+2e} [PtCl_4]^{2-} + 2Cl^-$$

$$[PtCl_4]^{2-} \leftrightarrow Pt^{2+} + 4Cl^-$$

$$NaHCO_3 \leftrightarrow Na^+ + HCO_3^-$$

$$Na_2CO_3 + H_2O \leftrightarrow NaOH + NaHCO_3$$

$$NaOH \leftrightarrow Na^+ + HO^-$$

$$Na^+ + Cl^- \rightarrow NaCl$$

The reduction of $[PtCl_4]^{-2}$ to Pt(0) atoms proceeds in two steps: dissociation of Cl from $[PtCl_4]^{-2}$, and reduction of Pt^{2+} to Pt(0) atoms. In the second process, both Pt^{2+} and Pt(0) coexist in the solutions. Once a Pt(0)-Pt(0) bond is formed, the association of Pt(0) atoms into Pt(0)-Pt(0) oligomeric clusters is activated to create a Pt particle.

The electrochemical processes that take place at electrodes are:

$$\text{Cathode: } Pt^{2+} + 2e^- \rightarrow Pt^o$$

$$\text{Anode: } 2HO^- - 2e^- \rightarrow H_2O + 1/2O_2$$

The hypothesis of platinum nanoparticles formation was also verified by XRD analysis. The X-ray diffractograms (smoothed plots) of the obtained platinum nanoparticles

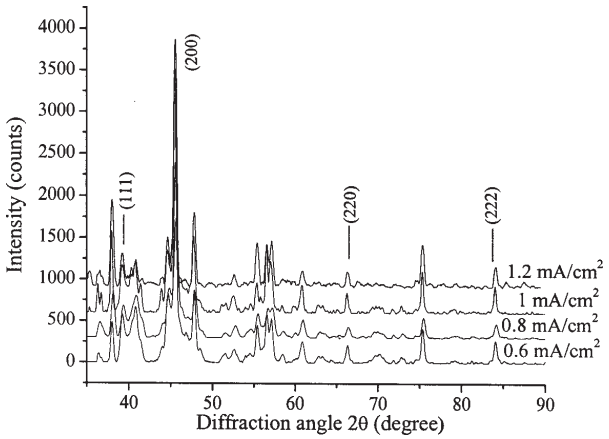

Fig. 4 The X-ray diffractograms of obtained platinum nanoparticles– PAmHU powders. The galvanostatic current regime is mentioned for every sample

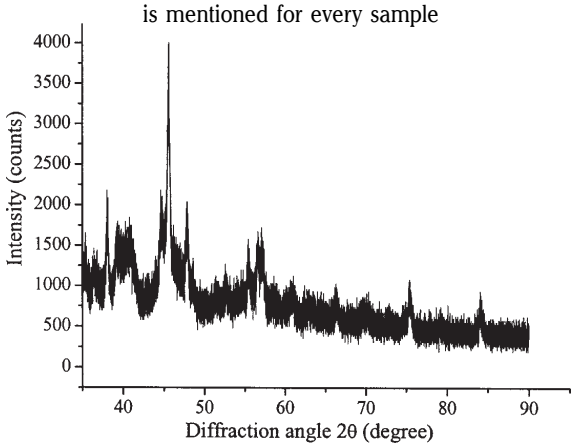

Fig. 5 The pristine X-ray diffractogram of obtained platinum nanoparticles– PAmHU powders at 1.2 mA/cm^2 current density

are presented in figure 4. The 2θ peaks at 39.275°, 45.668°, 66.569° and 84.465° are attributed to the crystal planes of platinum at (111), (200), (220) and (222), respectively [25].

The existence of Pt nanoparticles can be proved by the broad bands in X-ray pattern spectra. This behaviour is due to the breaking in symmetry of vicinal surfaces with the nanocrystal dimensions and with the interfacial strains. If the breadth is consistent for each peak, then certainly, the broadening is due to crystallite size as can be seen in figure 5 for 1.2 mA/cm^2 current density, while, on the contrary it can be due to defects of mechanical transmission or detection limit of diffractometer.

The crystallite sizes calculated with Scherrer equation (1) are presented in Table1. The obtained structures have a varied geometric configuration, this being also confirmed by AFM studies.

Figure 6 shows the 2D and 3D AFM topographies, and the phase contrast for films of PAmHU and platinum nanoparticles suspensions. The values of nanoparticles size are higher than those obtained from XRD diffractograms, suggesting that platinum nanoparticles are capped by polymer.

Table 1
THE DIMENSION (NM) OF PLATINUM CRYSTALLITES CALCULATED WITH SCHERRER RELATIONSHIP

2θ (hkl)	39.275 (111)	45.668 (200)	66.569 (220)	84.465 (222)
0.6 mA/cm^2	10.74	17.66	22.1	23.25
0.8 mA/cm^2	10.36	13.18	16.57	20.18
1 mA/cm^2	11.68	23.04	29.83	30.93
1.2 mA/cm^2	23.66	32.23	40.03	41.96

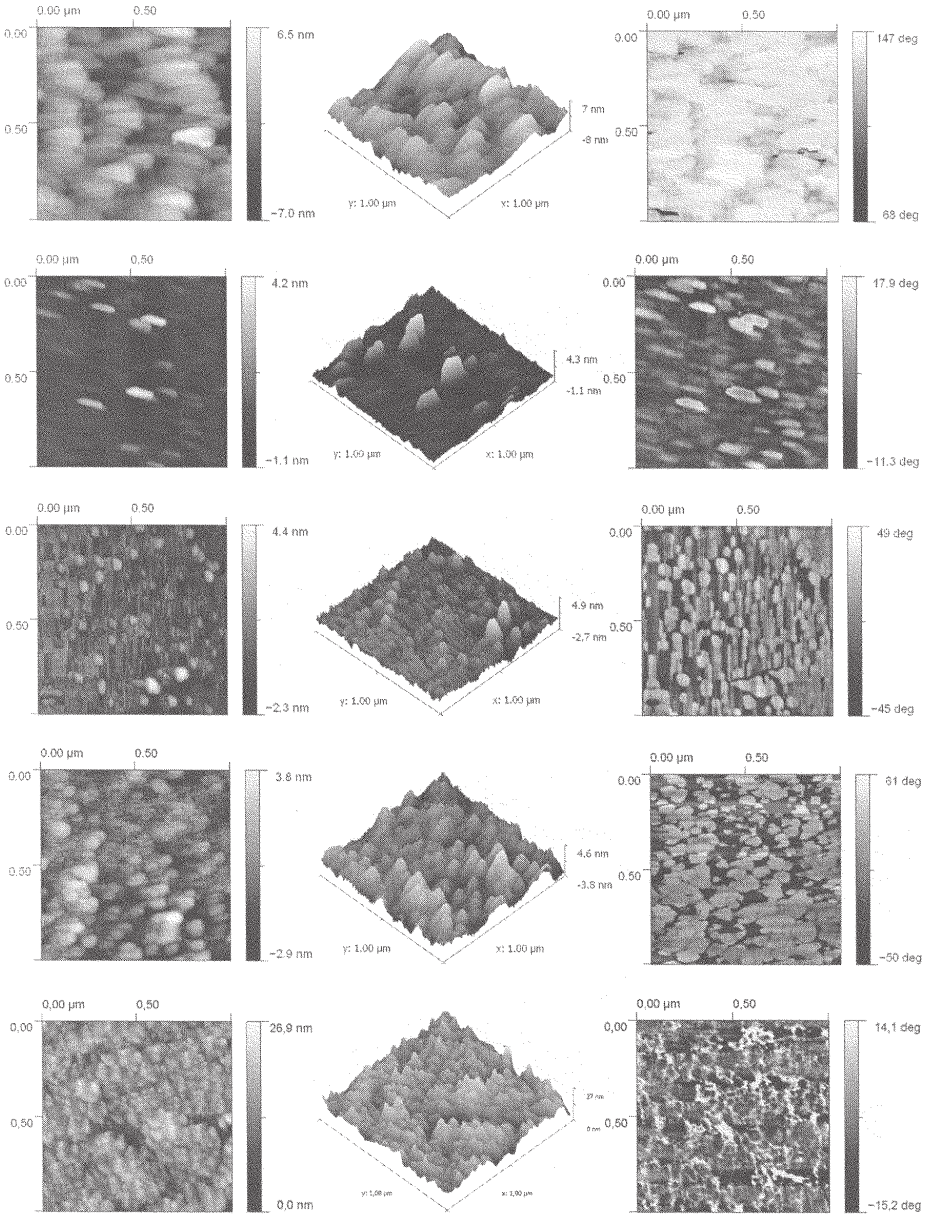

(a) *(b)* *(c)*

Fig. 6 The 2D (a) and 3D (b) topographies and phase contrast (c) for films of PAmHU and platinum nanoparticles suspensions obtained at 0.6 mA/cm^2, 0.8 mA/cm^2, 1 mA/cm^2 and 1.2 mA/cm^2 current densities (from top to bottom); the scale of square area is 1 x 1µm^2

From the size distribution diagram (fig. 7) it results that the PAmHU polymer presents a micelle to coil structure [16], with two different distributions: one having its maximum at 77.5 nm and the other at 654 nm. For current values of 0.8 and 1 mA/cm^2 three distributions appear. Light scattering simulations using Mie theory for the distributions value with the highest ponderosity, considering these are given by Pt nanoparticles, are in good agreement with experimental results of UV-Vis spectra deconvolution (as shown in fig. 3). For the other distributions, with the smaller nanoparticles sizes, the simulations showed no concordance with experimental results. These observations permit us to affirm that the distributions are given by PAmHU packed structure whose sizes are determined by electrolyte ionic strength and the condition of local electrical field during the synthesis, this being accentuated by the distributions shifting to the smaller values of sizes with current density increasing. Regarding average values in table II it is shown that the syntheses at 0.8 and 1 mA/cm^2 current values are the worst, good results being obtained for low (0.6 mA/cm^2) and high (1.2 mA/cm^2) current densities for which the polydispersity index is slightly higher than 0.5.

The colloidal solutions stability is defined according to the average value of Zeta potential [26] (table 3). We must specify that the stability conditions defined in table III were established for suspension of spherical particles model, in which the affinity of the particle surface with water creates a structured surface water layer, and this structure changes considerably the properties of the particle – water – polymer from those in the bulk. This electrostatic field, in combination with the thermal motion of the ions, creates a countercharge, and thus it screens the electric surface charge. The net electric charge in this screening diffuse layer is equal in magnitude to the net surface charge, but has the opposite polarity.

From the Zeta potential distribution (fig. 8) we conclude that micelle to coil structures are negatively charged, showing that the N-H functional groups of urethane bond and from acrylamide are almost complete deprotonated. The PAmHU presents three maximums at: -39.5 mV, -19.7 mV and -0.365mV. Zeta potentials for platinum nanoparticles show the existence of a stable fraction and one that by flocculation can deposit on the bottom of vessel.

Comparing the average values of Zeta potential from table II of nanoparticles assembly obtained at previous mentioned parameters of synthesis with stability condition expressed in table III it can be observed that the polymer has a moderate stability (ZP = -25.3 mV) and thereby it was expected the Pt nanoparticles to have a stability

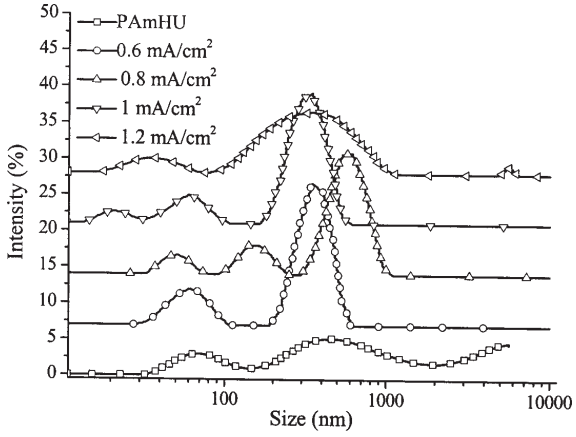

Fig. 7 The size distribution of PAmHU polymer domains and PAmHU – Pt nanoparticles systems obtained at different values of current density

Table 2
CHARACTERISTICS OF COLLOIDAL SUSPENSIONS BEHAVIOUR

Sample	Average size (nm)	Polydispersity	Average Zeta potential (mV)	Zeta deviation (mV)	Conductivity (mS/cm)
1.2 mA/cm^2	341	0.475	-18.2	20.5	3.44
1 mA/cm^2	382	0.555	-14.9	20.0	3.48
0.8 mA/cm^2	989	0.942	-3.42	32.4	3.49
0.6 mA/cm^2	501	0.592	-16.1	21.8	3.55
PAmHU	324	0.860	-25.3	15.8	3.37

Table 3
COLLOIDAL SOLUTIONS STABILITY – ZETA POTENTIAL RELATION (AFTER THOMAS RIDDICK - "A CONTROL OF COLLOIDAL STABILITY" [26])

Stability	Average Zeta potential (mV)
Extreme to very good stability	–100 to –60 mV
Reasonable stability	–60 to –40 mV
Moderate stability	–40 to –30 mV
Threshold of light dispersion	–30 to –15 mV
Threshold of agglomeration	–15 to –10 mV
Strong agglomeration & precipitation	–5 to +5 mV

bellow that value. We can notice that the less stable Pt nanoparticles are those obtained for current values of 0.8 and 1 mA/cm^2, which are situated at the superior limit of agglomeration threshold. The better results were obtained for low (0.6 mA/cm^2) and high (1,2 mA/cm^2) current densities, that are situated at the inferior limit of the dispersion threshold by the Zeta potential average values.

In the previous *ad literam* characterization we must consider that the Zeta potential average values were calculated for the spherical particles model presented, for which the potential distribution presents only one maximum and the true value of Zeta potential should be higher in absolute value, this being proved by the fact that the solutions are stable for more than 6 months.

Also, presence of the platinum nanoparticles [27] is proved by the conductivity of final solution compared with PAmHU (Table II). It is known that non-conducting particle reduces the total current going through the conducting medium because the conducting liquid is replaced with non-conducting particles and *vice versa* a conducting particle increases the total current. From this point of view, the higher the galvanostatic current at which were obtained, the less conducting the capped Pt nanoparticles are.

In order to confirm the bonding of PAmHU polymer with platinum nanoparticles, the FTIR spectra of PAmHU and PAmHU-Pt nanoparticles system were investigated. Information about the characteristic IR bands of PAmHU is presented in [16].

The characteristic bands of PAmHU functional group region (fig. 9a) and fingerprint region (fig. 9b), corroborated

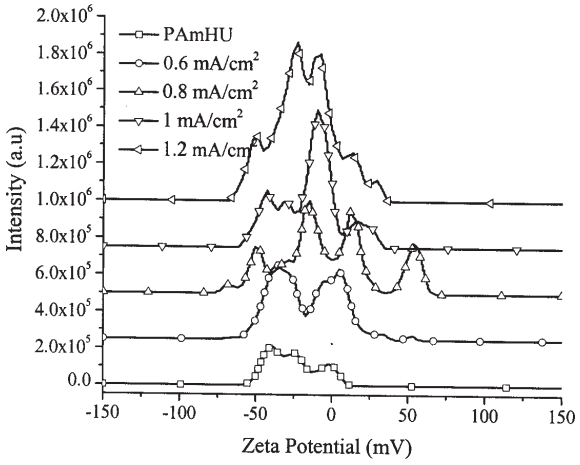

Fig. 8 Zeta potential for PAmHU polymer and PAmHU – Pt nanoparticles systems obtained at different values of current density

with correlation chart reveals that the regions of water absorption at 3600 – 2800 cm^{-1} and 1750 – 1550 cm^{-1} are strongly affected by the presence of platinum nanoparticles.

These bands are given by the fundamental stretching vibrations mode of water (they occur within the 3900–2800 cm^{-1}) and deformation vibrations of O – H groups in water (the in plane bending mode at around 1620 cm^{-1}).

The broad band 3600 – 3200 cm^{-1} specific to O – H vibrations stretching could be drastically affected by the population of water bonded by the interaction of the electron pairs of oxygen with positive metal platinum

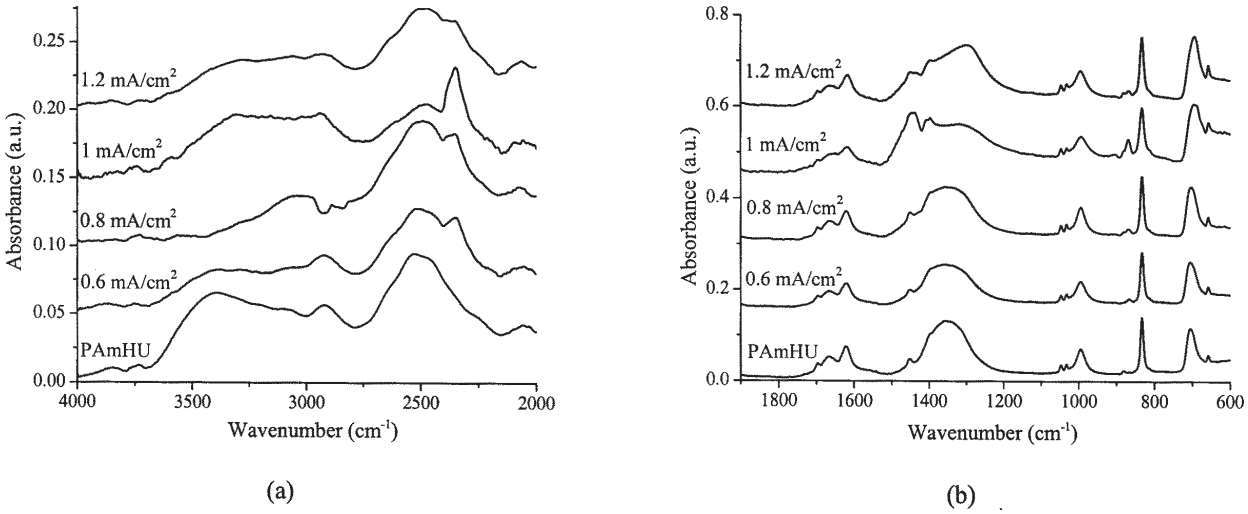

Fig. 9 FTIR spectra for PAmHU polymer and polymer capped Pt nanoparticles; functional group region (a) and fingerprint region (b)

surface or by dipole – charge interaction and, at the other end being the water – PAmHU hydrogen bond, probably from the three possible proton acceptors groups: the ether oxygen, the urethane carbonyl oxygen, and the acrylamide carbonyl oxygen. As a result, the amide broad band 2770 – 2160 cm^{-1} changes its profile. The peak at 1698 cm^{-1} due to vibrations of free C = O from urethane groups (hard segment), and the shoulder at 1680.67 cm^{-1} assigned to carbonyl groups involved in H bonding with the N – H groups of the urethane hard fragments seems to be slightly affected. It is also important the broad band 1450 – 1200 cm^{-1} that contain the wag mode at 1448 cm^{-1} of C – O – C and CH_2 bands from ether and ethyl respectively (soft segment); C – H band and O – H band that changes its contribution due the new folding possibility by the presence of the Pt nanoparticles.

Changes will be given also by the anions salts dissociation that exist in solution and thermally diffuse in the negatively charged diffuse layer as free ions or complexes with PAmHU.

Conclusions

Platinum nanoparticles have been synthesized by sonoelectrochemical method in the presence of poly(amidhydroxyurethane). The sizes of platinum crystallites obtained from X-ray diffractograms are in the range of 10-42 nm. The dimensions obtained from AFM and size distribution studies are higher than those from X-ray diffractograms, suggesting that nanoparticles are capped by PAmHU macromolecules. This fact is confirmed by FTIR analysis. From the analysis of average Zeta potentials it results that for certain electrochemical synthesis conditions the colloidal systems obtained – PAmHU capped platinum nanoparticles – are in stability limit.

Acknowledgements: This study was financially supported by PN II Idei 509/2008 and PN II Td 24/2008 scientific research projects in the frame of the Romanian MEC Programme.

References

1.HIRAI, H.; CHAWANYA, H.; TOSHIMA, N., React. Polym., **3**, 1985, p. 127
2.COLVIN, V.L.; SCHLAMP, M.C.; ALIVISATOS, A.P., Nature, **370**, 1994, p. 354
3.WANG, M.Q., DU, X.Y., LIU, L.Y., SUN Q., JIANG X.C., Chinese J. Anal. Chem., **36(7)**, 2008, p. 890
4.PARFENOV, A., GEDDES, C.D., LAKOWICZ, J.R., J. Fluoresc., **13(4)**, 2003, p. 297
5.TURKEVICH, J., KIM, G., Science, **169**, 1970, p. 873
6.MELNIG, V., APOSTU, M.O., FOCA, N., J. Nanopart. Res., **10**(SUPPL. 1), 2008, p. 171
7.TORIGOE, K., ESUMI K., Langmuir, **9**, 1993, p. 1664
8.BRADLEY, J.S., HILL, E.W., KLEIN, C., CHAUDRET, B., DUTEIL, A., Chem. Mater., **5**, 1993, p. 254
9.BOWLES, R.S., KOLSTAD, J.J., CALO J.M., ANDRES, R.P., Surf. Sci., **106**, 1981, p. 117
10.CHMIELEWSKI, A.G., CHMIELEWSKA, D.K., MICHALIK, J., SAMPA, M. H, Nucl. Instrum. Methods B**, 265(1)**, 2007, p. 339
11.OBREJA, L., DOROHOI, D.O., MELNIG, V., FOCA, N., NASTUTA, A., Mat. Plast., **45**, no.3, 2008, p. 261
12.OBREJA, L., FOCA, N., POPA, M.I., MELNIG, V., Scientific Annals of "Alexandru Ioan Cuza din Iaşi" University, **Tomul I**, s. Biomaterials in Biophysics, Medical Physics and Ecology, 2008, p. 31
13. CISMARU, L., HAMAIDE, T., POPA, M., Mat. Plast., **44**, no.3, 2007, p. 243
14.DUFF, D.G.; EDWARDS, P.P.; JOHNSON, B.F.G., J. Phys. Chem., **99**, 1995**,** p. 15934
15.MIZUKOSHI, Y., OSHIMA, R., MAEDA, Y., NAGATA, Y., Langmuir**, 15**, 1999, p. 2733
16.MELNIG, V., CIOBANU, C., J. Optoelectron. Adv. Mater., **7(6)**, 2005, p. 2809
17.SCHERRER, P., Göttinger Nachr, .**2,** 1918, p. 98
18.*** http://www.philiplaven.com/mieplot.htm
19.*** http://refractiveindex.info
20.HENGLEIN, A., ERSHOV B.G., MALOW M., J. Phys. Chem., **99**,1995, p. 14129
21.SWIHART, D.L.; MASON, W.R., Inorg. Chem., **9**, 1970, p.1749
22.CREIGHTON, A, EADON D.G. J. Chem. Soc. Faraday Trans., **87**, 1991, p. 3881
23.VANYSEK, P, CRC handbook of chemistry and physics, 68th ed. CRC Press, ed. Weast, R. C., Boca Raton, Florida, 1991, p. D-151 1987
24.CAMERON, R.E.; BOCARSLY, A.B., Inorg. Chem., **25**, 1986, p. 2910
25.HAGLUNG, J., FERNANDEZ-GUILLERMET, A., GRIMVALL, G., KORLING, M., Phys. Rev. B, **48**, 1993, p. 11685
26.RIDDICK, T.M., Control of Colloid Stability through Zeta Potential, Copyright © 1968 by Thomas M. Riddick Library of Congress Catalogue Number 67–18001
27. MELNIG, V., APOSTU, M.-O., FOCA, N., Mat. Plast. **46**, no. 3, 2009, p. 274

Manuscript received: 13. 04.2009